Computational fluid dynamics and performance evaluation of a chimney solar dryer for chilli pepper

Francis Kumi[1], Bram Parbi[1], Robert Sarpong Amoah[1], Jonathan Ampah[2]

(1. Department of Agricultural Engineering, School of Agriculture, College of Agriculture and Natural Sciences, University of Cape Coast, Cape Coast, Ghana.

2. CSIR-Food Research Institute, P.O.Box M20, Accra, Ghana)

Abstract: The postharvest losses of agricultural produce in Ghana and other developing countries is high. Efforts to promote shelf-life extension of the fresh products is centred on temperature and moisture management. Moisture control by drying is suited to a number of crops as it inhibits microbial decay and physiological processes of deterioration. However, efficient drying infrastructure is often unavailable to farmers in developing countries. Thus, the focus of this research was to structurally modify a chimney solar dryer originally designed by the Horticulture Innovation Laboratory of the University of California, Davis and include sea pebbles in the collector base to enhance its heating system and drying performance. A computational fluid dynamics analysis using ANSYS FLUENT was used to assess the functional parameters such as the airflow, temperature and relative humidity. Subsequently, the performance of the modified dryer was compared with the original design using chilli pepper (*Capsicum annuum* L.) as the test product. The results showed a strong correlation between the simulated and no-load experimental conditions in terms of temperature (R= 0.987) and relative humidity (R = 0.927). The presence of sea pebbles improved the drying rate, reducing the moisture content of the chilli from 73.12% to 7.15% (w.b.) in 36 h, while without sea pebbles, the chilli dried to 9.67% (w.b.) within the same period. Overall, the inclusion of sea pebbles and the minor structural modification enhanced the drying performance of the chimney solar dryer.

Keywords: chimney, dryer, computational fluid dynamics, simulation, moisture content.

Citation: Kumi, F., B. Parbi, R. S. Amoah and J. Ampah. 2022**.** Computational fluid dynamics and performance evaluation of a chimney solar dryer for chilli pepper. Agricultural Engineering International: CIGR Journal, 24(2): 153-165.

1 Introduction

There is high postharvest loss of fruit and vegetables in sub-Saharan Africa (Sheahan and Barret, 2017; Affognon et al., 2015). Specifically, farmers lose between 30 % - 40 % of the value of their fruits and vegetables before they get to the final consumer (Kumar et al, 2006; Korsten, 2006). Chilli pepper is cultivated in every region of Ghana and is largely consumed as an ingredient in staple foods. High losses are encountered during the glut season (Shitanda and Wanjala, 2006) and farmers are unable to meet off-season market demands. These losses could be attributed to the unavailability of suitable drying technologies to aid the shelf life extension of the produce.

In contrast, there is abundant solar energy in the tropical developing countries which offers immense opportunities to develop appropriate drying technologies for drying agricultural products. Despite this, most rural farmers still practice open-sun drying which has limitations such as longer drying times and food contamination (Shitanda and Wanjala, 2006). From the economic and technical perspectives, solar drying tends to be the more appropriate alternative for crop drying in rural communities in developing countries (Poonia et al.,

Received date: 2020-09-04 **Accepted date:** 2021-07-17

***Corresponding author: Francis kumi**, Senior Lecturer, Department of Agricultural Engineering, School of Agriculture, College of Agriculture and Natural Sciences, University of Cape Coast, Cape Coast, Ghana, Phone: +233-553135913, Email:francis.kumi@ucc.edu.gh.

2019; Bala and Janjai, 2009). It is therefore imperative to provide appropriate solar drying solutions to sustain all-year-round availability of farm produce to enhance food security and improve the livelihood of farmers.

Drying involves heat and mass transfer between products and the surrounding air; therefore, the effectiveness of the solar drying process is much dependent on the optimized environmental conditions, particularly temperature and relative humidity of the air. A high temperature and a low relative humidity promote drying rate. Controlling these parameters require close monitoring by installing several sensors at different locations in the dryer. This process control method could be expensive. Thus, a more economical approach is the use of numerical and simulation models to predict the performance of dryers. In line with this, several studies have relied on modelling and simulation as a tool to optimize the drying rate of agricultural products (Demissie et al., 2018; Odinaka and Akubue, 2018). Computational fluid dynamics (CFD) method has been accepted as an effective tool for numerical simulations of such systems, predicting the flow behaviour and mass transfer phenomena occurring in multi-component systems in many industries (Sanghi et al., 2018).

In the current study, a chimney solar dryer was simulated by computational fluid dynamics method and employing ANSYS Fluent software. Also, the drying process of chilli pepper was evaluated in the solar dryer.

2 Materials and Methods

2.1 Modifications and CFD modelling

2.1.1 Modifications

The solar chimney dryer in this study was originally designed by the Horticulture Innovation Laboratory of the University of California, Davis in the United States of America (Deltsidis et al., 2018). Our initial collaboration with this institution led to the construction of a prototype and evaluation of its performance in comparison to open sun drying. The results showed better dryer performance than open sun drying (Kumi et al., 2020). However, further studies of the prototype established the need for structural modifications to further improve the performance, particularly by enhancing the heating system. As a modification to achieve higher efficiency, a permanent tunnel was constructed and affixed on top of the collector. This modification allowed access to only one side of the tunnel for the periodic removal of the drying trays instead of taking off the whole transparent polythene sheet draped over the horizontal bar. By experience and general observation, it was realised that sea pebbles are able to retain heat energy for long periods during sunny days. This provided an innovative opportunity to place them inside the collector chamber to enhance the heating system in order to increase the rate of drying.

The modified dryer is mainly composed of a heat collector containing sea pebbles, a drying chamber, drying trays, and a chimney for moisture outlet. Figure 1 shows the drawings of the collector table (a), drying tray (b) and the chimney (c). Figure 1(d) shows the three-dimensional assembly drawing of the modified chimney solar dryer drawn using Solid works 2017 (Dassault Systèmes SOLIDWORKS Corporation, Waltham, Massachusetts, USA).

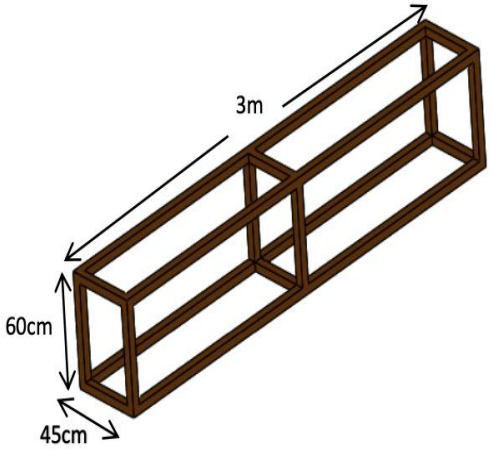

(a) Frame of the solar collector table

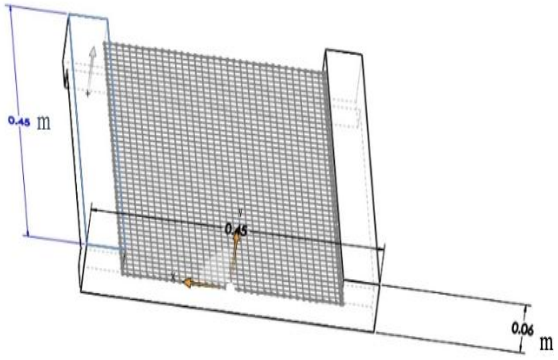

(b) Drying tray with wire mesh

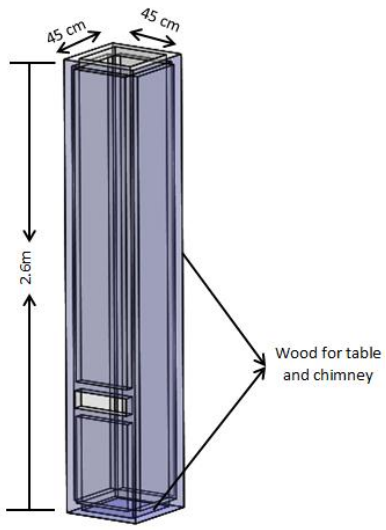

(c) Chimney covered with plain polythene plastic material

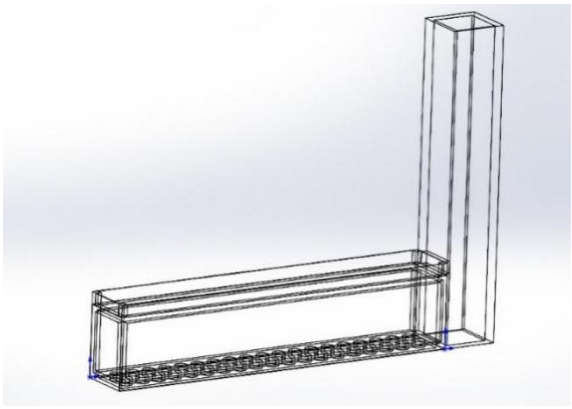

(d) Modified chimney solar dryer showing the sea pebbles at the collector base

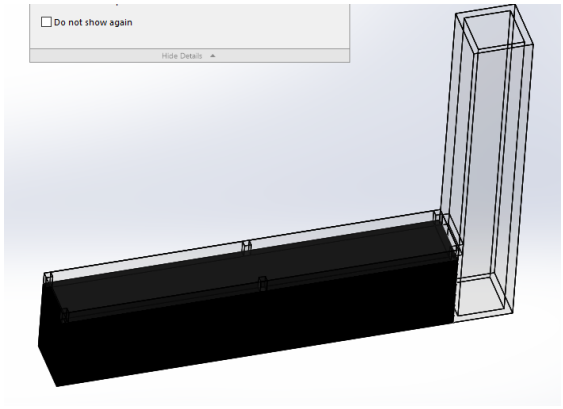

(e) Modified chimney solar dryer showing the collector covered with black material].

Figure 1 Drawings of the modified chimney solar dryer

2.1.2 CFD modelling

The design in SolidWorks was saved in IGS file format and imported into ANSYS FLUENT version 19.4 (ANSYS, Inc., Canonsburg, Pennsylvania, USA) for further processing, analysis and simulation. The global solar position of the sun was computed based on the latitude (5.11 ℃N) and longitude (1.29 ℃W) for the experimental location. The mesh size was determined after checking the orthogonal and skewness of the model. The mesh was generated based on medium relevance center and has 47677 nodes and 125578 elements. The grid was refined to confirm mesh independence. To identify mesh independency, the simulation was proceeded from coarse to fine mesh and the variation of the desired simulation output was checked. It is also possible to have mesh independent solution by using a very fine uniform mesh. However, it would take days/months to end the simulation process and thus, the simulation of this study was conducted on medium mesh. The discrete ordinate ray tracing method was used and solar load was used in ANSYS FLUENT. Figure 2 shows the meshed dryer model.

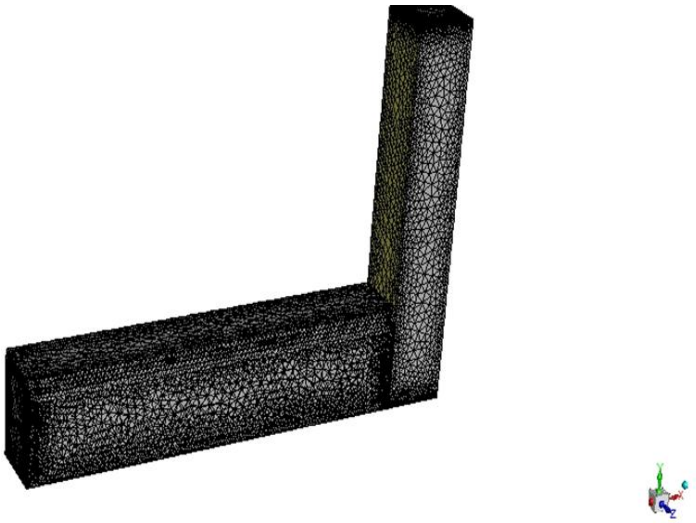

Figure 2 Meshing of the solar dryer using ANSYS FLUENT

An inlet air velocity of 1.4 m s^{-1} was used in the analysis. The direction of air flow was parallel to that of the dryer inlet and assumed to be at ambient temperature. A polythene sheet with 4 mm thickness and transmissivity of 0.9 mm was used and the effect of the wire net placed underneath the polythene sheet was assumed to be negligible.

The mixed type thermal conditions were used since heat flow within the dryer was by convection and radiation (surface to surface). Initial values for parameters such as air velocity, temperature, and relative humidity were selected, recorded and deployed. Transient calculation method was chosen and run. The simulation was performed at one (1) hour intervals from 9:00 am to 5:00 pm. Contours were generated at the end of the drying process. The key properties of the materials

used in the study are shown in Table 1.

Table 1 Key material properties used in the study

Materials/ Properties	Air	Polythene Sheet	Stones
Density (kg m^{-3})	1.225	0.941	2.6
Specific Heat (J $kg^{-1}K^{-1}$)	1005	1900	710
Viscosity (kg m^{-1} s^{-1})	2.8e-05	–	–
Thermal Conductivity (W m^{-1} K^{-1})	0.024	0.43	2.56

Note: Alonge and Obayopo (2019), Engineering ToolBox (2003), GoodFellow (2008)

2.2 Construction of the dryer

The general design consideration of the dryer includes the air inlet and outlet, solar collector, chimney and trays for holding the food materials. The drying table was made of wood covered by a net and polythene material. In this model, however, sea pebbles were placed on a plywood at the base of the collector table. Also, the top of the collector had a rectangular framework with one side closed and the other side locked with hinges that can be opened to place and remove trays from time to time. The air inlet was rectangular in shape to allow free flow of air into the dryer. This modification was carried out to reduce the heat loss experienced when a whole length of plain polythene bag was draped over the collector table during drying and also to ensure free air flow. Also, the chimney was covered with plain polythene bags at the bottom and all the four sides. The trays (made of wood and wire meshes) were placed on top of the collector table.

(a) Experimental set-up for the performance evaluation – left: The original dryer, right: - modified dryer (b) The collector base of the modified dryer containing sea pebbles

Figure 3 Constructed Chimney solar dryers

2.3 Experimental procedure

The experiment was carried out at the A.G. Carson Technology Centre of the University of Cape Coast, Ghana in January 2020. The mean annual rainfall at the location is between 750 and 1500 mm. The average temperature in the area usually ranges from 24 ^{o}C to 29 ^{o}C.

2.3.1 No load experiment

The no load experiment was conducted in January, 2020 prior to the load experiments. This test was conducted to determine the temperature, relative humidity and air velocity in the dryer. Temperature and relative humidity were recorded hourly from 9:00 am to 5:00 pm.

2.3.2 Load experiment

Freshly harvested chilli pepper (Legon 18 variety) was obtained from a Ministry of Food and Agriculture (MoFA) accredited farmer at Cape Coast in the Central Region of Ghana. Afterwards, the pepper was sorted and washed. Then 320 g of that was spread on each dryer tray. The performance of the modified dryer with sea pebbles were compared to the original dryer without sea pebbles (Figure 3). Also, a clear polythene material was draped around a horizontal bar at the top of the collector table of the original dryer to create a tunnel for air circulation.

The initial moisture content of the pepper was determined using the oven drying method at a temperature of 105 ℃ till a constant weight was obtained as reported by Turhan et al. (1997).

During the testing period, the temperature and relative humidity of ambient and dryer collector were

measured by HTC-1 Temperature and humidity sensors (Figure 4 (a)). The weight loss in the designed dryer and that of the control were determined every four hours with an electronic weighing balance (Radwag WTC 2000) having maximum load measurement of 2000 g and an accuracy level of 0.01g. The weight loss at each point of measurement was used to calculate the corresponding moisture content based on the initial moisture content. Drying was carried out for eight hours daily. The effective performance of the dryer was assessed by calculating the solar dryer performance coefficient, drying rate and moisture ratio. The UC-Davis dry card (Figure 4(c)) was used to determine the appropriate time to end the drying process.

(a) Temperature and humidity sensor

(b) Handheld anemometer

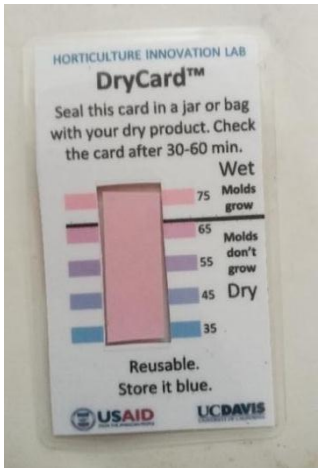

(c) dry-card

Figure 4 Instruments used in the experiment

2.4 Moisture ratio

The moisture ratio (MR) was determined using the following formula:

$$MR = \frac{M - M_e}{M_i - M_e} \quad (1)$$

Where, M is the moisture content (dry basis) at some time, M_e is the equilibrium moisture content (dry basis), and M_i is the initial moisture content (dry basis).

2.5 Effective moisture diffusivity

For the determination of the effective moisture diffusivity (D_{eff}), reference was made to Fick's second law of diffusion and its model expressed in Equation 2:

$$MR = \frac{8}{\pi^2} exp[\frac{\pi^2 D_{eff}}{4l^2} t] \quad (2)$$

Where, MR is moisture ratio (no units), D_{eff} is effective moisture diffusivity ($m^2\ s^{-1}$), t is the drying time (s), l is the thickness (m) (in most cases, half the thickness of the sample – assumed to be 0.003 m in this work).

Taking the natural logarithm (ln) of both sides of Equation 3 results in Equation 3

$$In(MR) = In\left[\frac{8}{\pi^2}\right] - \left[\frac{\pi^2 D_{eff}}{4l^2} t\right] \quad (3)$$

When $ln(MR)$ is plotted against the drying time, t, a straight line with a negative slope, K, could be obtained where:

$$K = \frac{\pi^2 D_{eff}}{4l^2} \quad (4)$$

2.6 Solar dryer performance coefficient (DPC) and drying rate

The DPC is an effective parameter for assessing the performance of dryers (Itodo et al., 2019). It is the ratio of the mean relative humidity of the air entering the dryer to the mean relative humidity of the air exiting the dryer over the drying period and is expressed as in Equation 5.

$$DPC = \frac{RH_a}{RH_e} \quad (5)$$

Where, RH_a is the mean relative humidity of the air entering the dryer throughout the drying period (%), RH_e is the mean relative humidity of the air leaving the dryer throughout the drying period (%).

2.7 Data analyses

The data was obtained from the simulation and experimental values in the two conditions of no-loaded and loaded dryer to determine drying rate of the chilli

pepper in the designed dryer (with sea pebbles) and its control dryer (with no sea pebbles). Data were subjected to two sample t-test analyses in Minitab software (Minitab, LLC, Pennsylvania, USA) version 17. Simple linear regression was also conducted as well as the Pearson correlation coefficient determined for the data.

3 Results and discussion

3.1 Simulation

Figure 5 shows a streamline of the direction of the airflow in the dryer. The dryer was designed in such a way that it allowed air from the ambient environment to move through the opening of the tunnel along a horizontally direction over the trays and picks up moisture from the product. Also, heat generated in the collector warms up the incoming air and causes it to rise through the tunnel, picks up more moisture and exits through the chimney as shown with red arrows. The pebbles inside the collector store heat energy which is released into the air to increase the rate of moisture removal from the product. Since the trays are all placed on the same horizontal level, there is uniform distribution of heat leading to uniformity in the drying of the product.

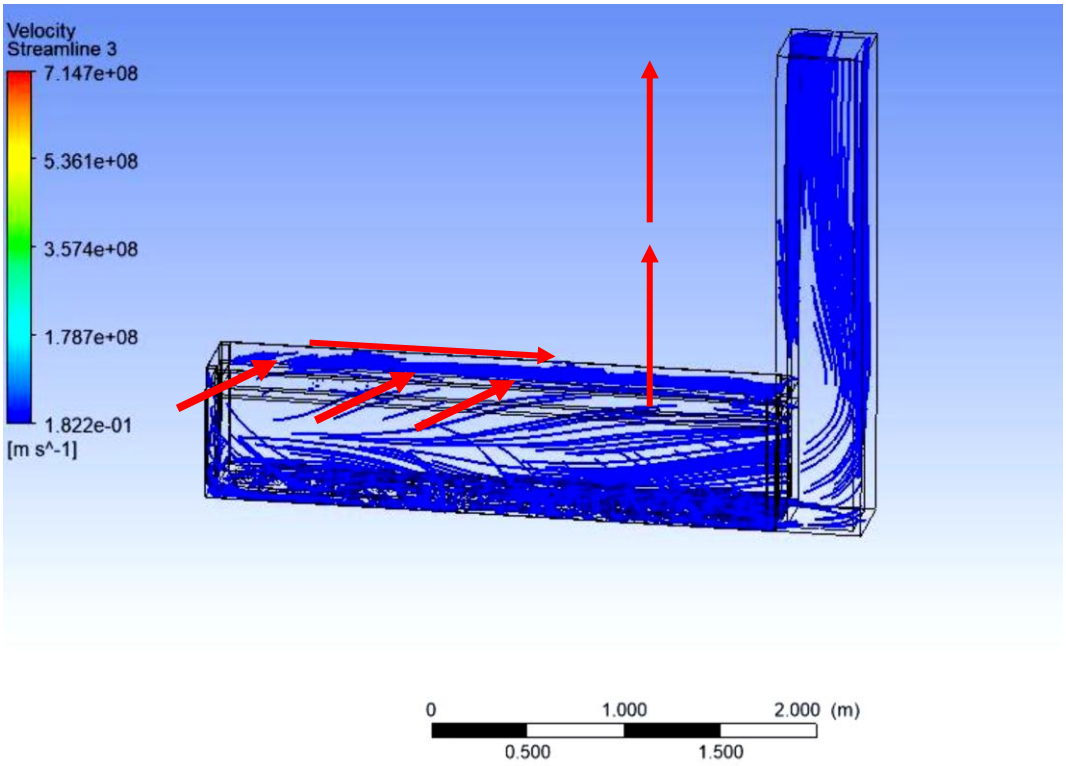

Figure 5 Streamline air flow pattern in dryer

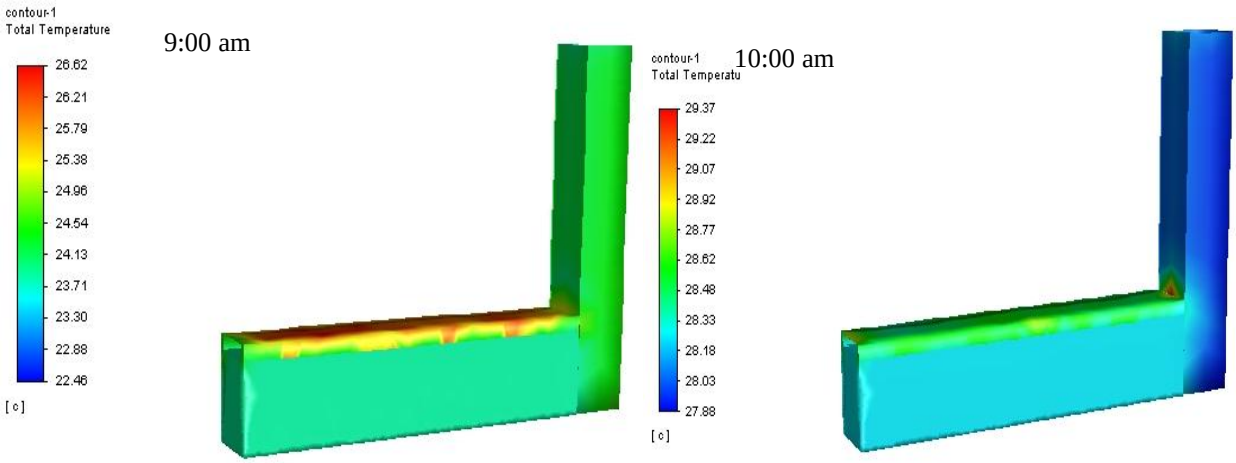

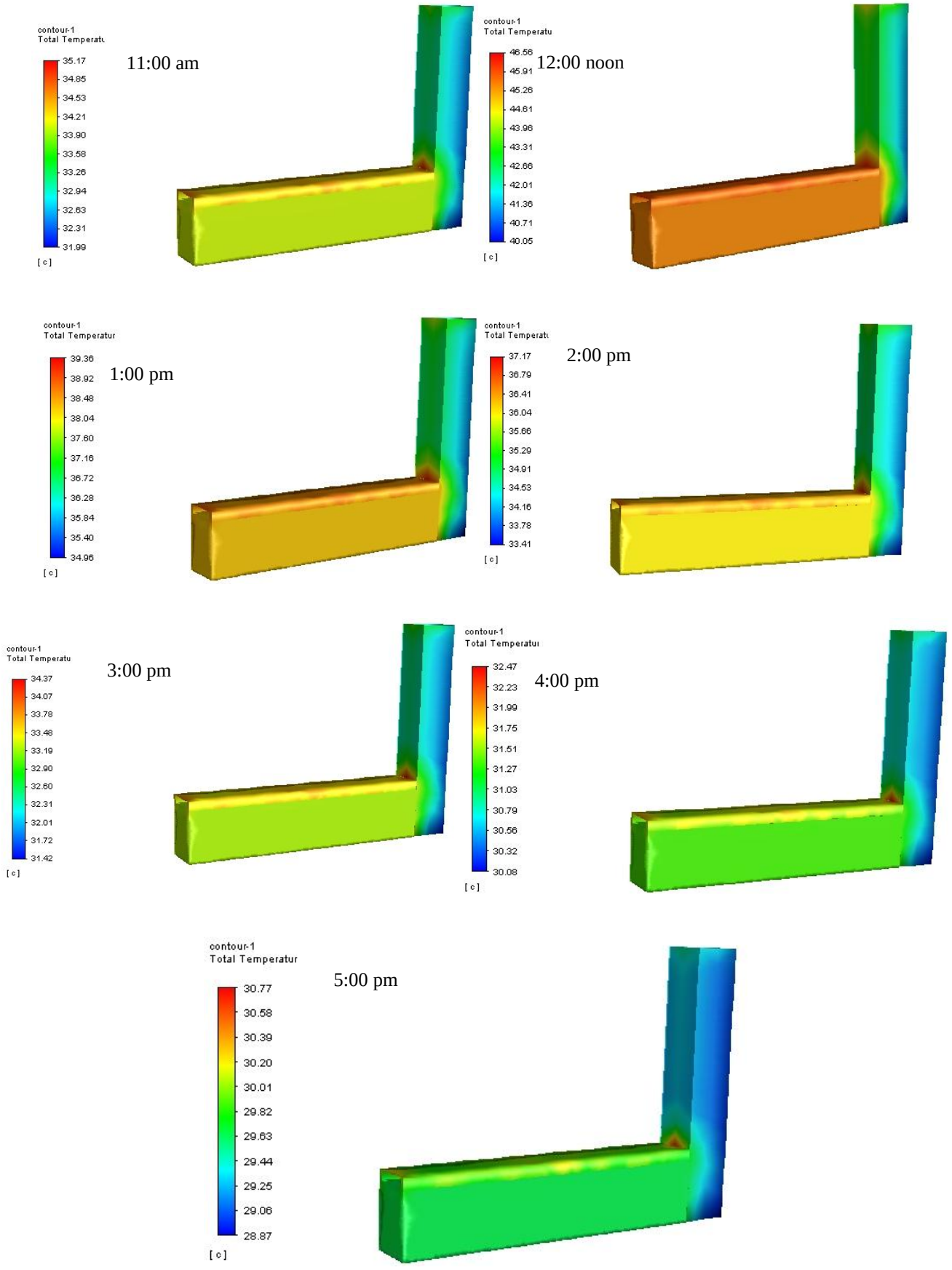

Figure 6 Temperature contours at specific times of the day

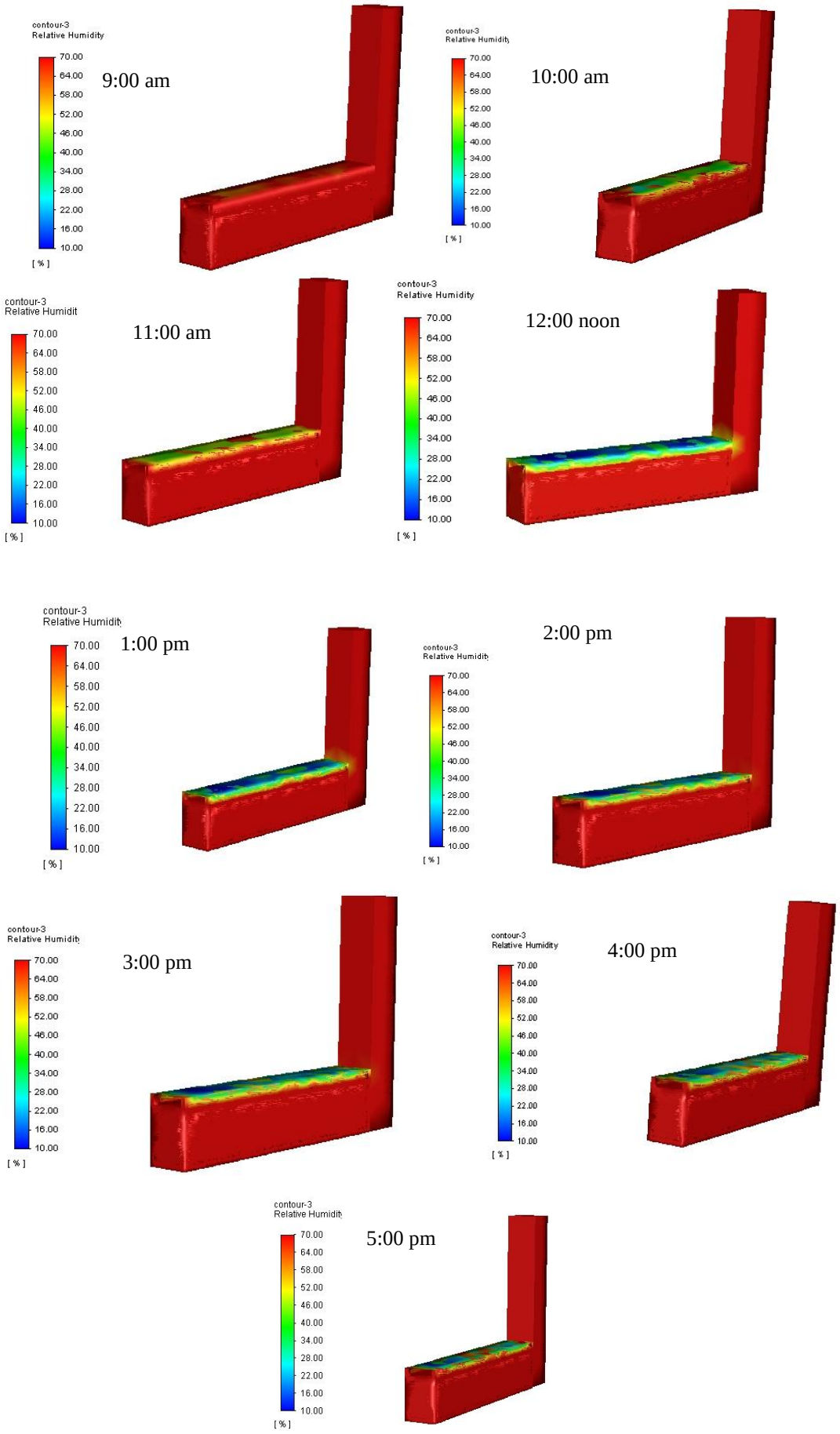

Figure 7 Relative Humidity contours in drying period

Figures 6 and 7 present temperature and relative humidity contours respectively in the dryer, throughout a day's drying period . It was observed that the maximum solar energy absorption occured at the base of the collector table which heats up the air and causes it rise into the tunnel, picking up moisture from the product. Mimimum absorption of solar energy was observed at the top of the tunnel even though it received the greatest solar irradiation. The temperature contours show that it was highest at 12 noon and lowest at 9 am and 5 pm, respectively. It could be concluded that the top of the collector where the trays were placed was thermally activated to enhance faster vaporisation of the moisture from the product. The transparent nature of the 4 mm thick polythene material enabled solar energy to penetrate through to the tunnel. This increased the heat energy required for moisture removal from the product.

Unlike the temperature contours, a reverse trend was observed for the relative humidity. Thus, while the highest temperature was recorded at 12 noon, its corresponding relative humidity was found to be the lowest. This trend shows that around this time of the day, under clear weather conditions, the dryer mostly experiences higher rate of drying and confirms the works of Kumi et al. (2020).

In principle, the contour tends to change in colour to show the variation in humidity over time. This tends to be one of the observational bases for predicting the changing moisture regimes in the dryer over time. The corresponding colour bar is the basis for estimating the values for both humidity and temperature and to show the actual trend of their distribution in the course of the drying period in a typical day of drying.

Empirical temperature data in no load drying condition and simulated data were compared. Figure 8 shows a positive regression between the simulated and empirical temperature data. The coefficient of determination was very high (R^2=0.974) and from the simple regression analysis, R^2 (adjusted), was found to be 0.970 which gives an indication of a strong relationship between the simulated and the actual experimental results under no load conditions. The correlation coefficient was also found to be 0.987 with a *p*-value of 0.000, which gives a high level of significance between the two parameters.

Figure 9 shows the relationship between the simulated and experimental relative humidities. In this case, the R^2 was found to be 0.86 with R^2 (adjusted) of 0.84 which also affirms a good linear relationship between the simulated and the experimental relative humidities. Furthermore, it gave a correlation coefficient (R) of 0.927 with a p-value of 0.000. This confirms the works of Sanghi et al. (2018) who found that the prediction of temperature using its simulated parameters tend to be stronger than that of the relative humidity of the same dryer. This was also confirmed by Demissie et al. (2018) who reported that there is a small (4.3^{O}C) average difference in the temperature between the simulated and experimental data. In another study by Janjai et al. (2008), it was reported that there is a strong correlation between the experimental and modelled temperatures using chilli pepper.

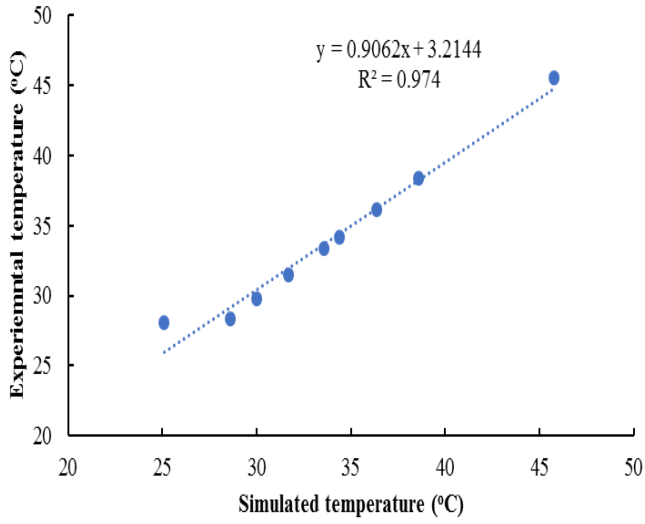

Figure 8 Simulated versus experimental temperature within the tunnel under no load conditions

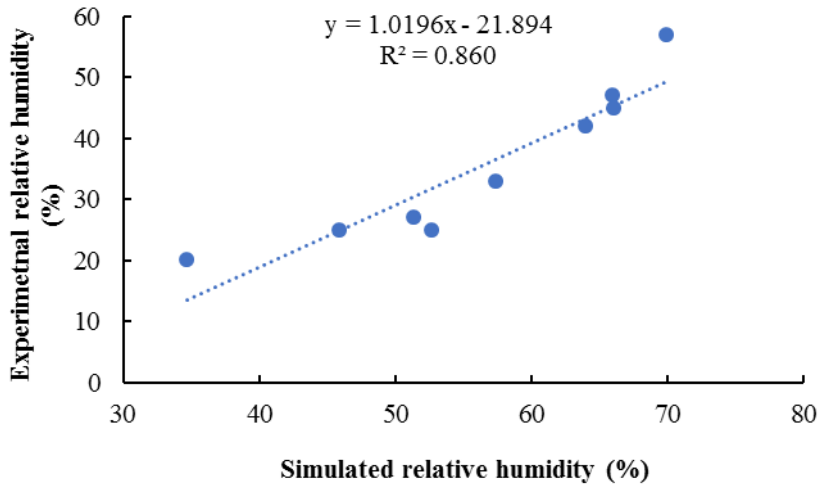

Figure 9 Simulated versus experimental relative humidity within the tunnel under no load conditions

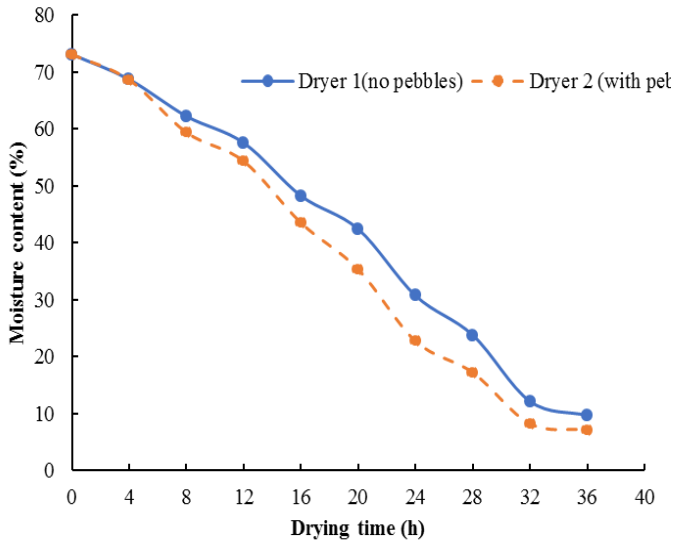

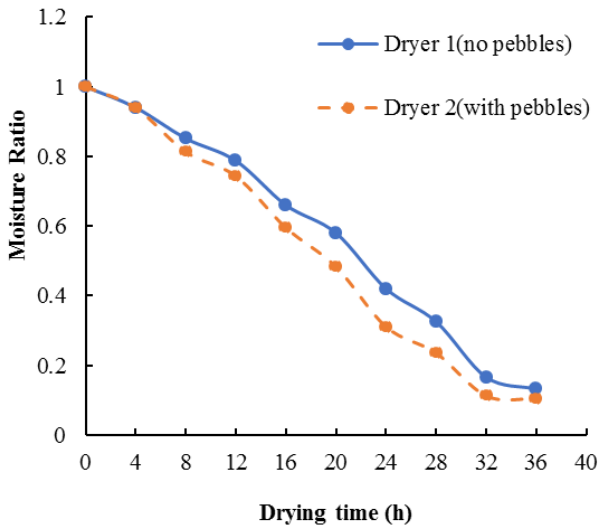

Figure 10 (a) Moisture content (% wet basis (w.b)) against time (h) Moisture ratio against time

3.2 Drying performance

3.2.1 Moisture removal and moisture ratio

From Figure 10 (a), there was a total of 36 h of solar drying for both dryers under comparative study and it was found that the dryer containing pebbles dried to a much lower moisture content at the end of the period than the one without pebbles. From an initial moisture content of 73.12 %, the dryer containing the pebbles dried to 7.15 % while the other dryer recorded 9.67 % after 36 h of exposure to the solar drying system. The corresponding moisture ratio is given in Figure 10 (b) depicting the same trend. This is in agreement with the works of others (Borah and Hazarika, 2017).

Overall, although there was no significant difference (p>0.05) in terms of the moisture content and moisture ratio data, it generally gives an indication that the sea pebbles enhanced the drying rate and could potentially shorten the time period needed to dry horticultural and other agricultural produce when incorporated into the design of solar dryers.

3.2.2 Effective moisture diffusivity

The graph showed straight line equations with negative slopes (Figure 11). It could be seen that there was almost a straight line on the $ln(MR)$ for the first 12 h after which the rate of moisture removal started falling (following a non-linear curve). Due to the fact that most of the drying occurred in the falling rate period, it is expected that mass transfer of bound water would be influenced by internal resistance. A similar observation was made and reported by Abano et al. (2011). Additionally, it could be observed that for a particular variety, the variations in $ln(MR)$ depend on temperature of drying air. The moisture diffusivity was found to be

8.93×10^{-8} m^2 s^{-1} and 1.061×10^{-7} m^2 s^{-1} for the dryer 1 (without pebbles) and dryer 2 (with pebbles), respectively. This gives an indication that the dryer with a relatively higher temperature gave a lower moisture diffusivity and vice versa.

The values obtained in this study fall within the recommended values reported by others for spices and food products (Borah and Hazarika, 2017; Abano and Amoah, 2015; Deshmukh et al., 2013).

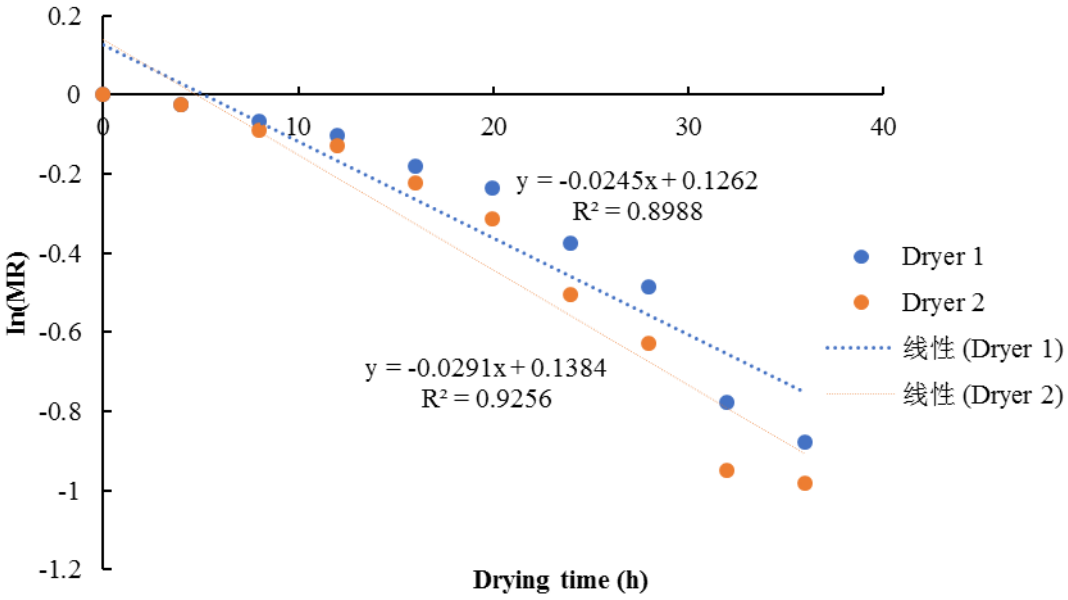

Figure 11 Variation of *ln*(*MR*) versus drying time

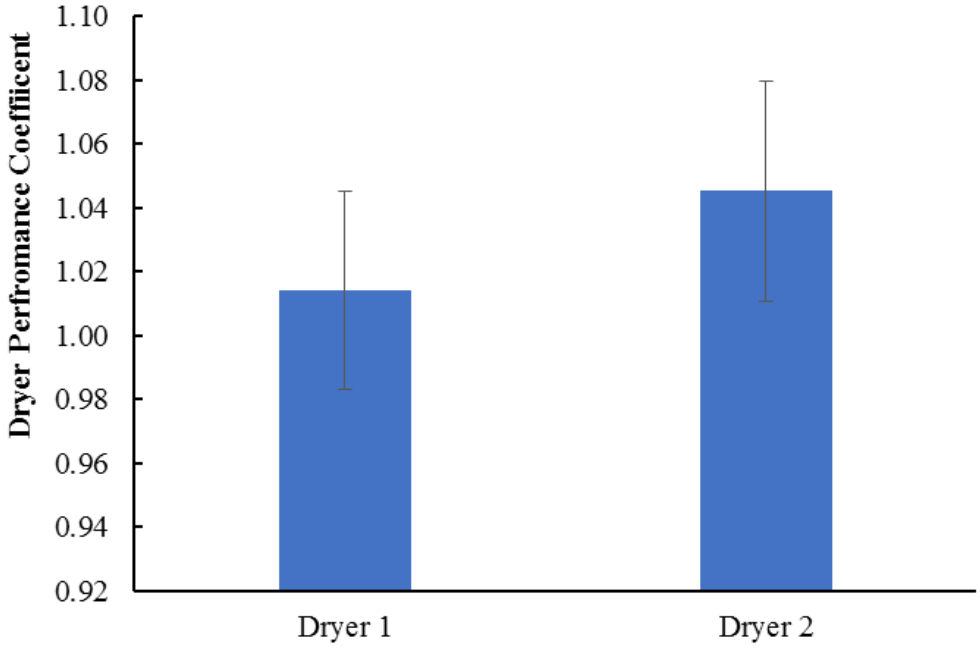

Figure 12 Dryer performance coefficient for the drying systems

3.2.3 Dryer performance coefficients

Figure 12 shows that the dryer performance coefficient (calculated using equation 5 above) of the dryer 2 (having pebbles) with a value of 1.05 was found to be higher than that of the original design (dryer 1 with no pebbles) having a performance coefficient of 1.01. Also, the mean drying rate over the 36 h of drying for the dryer 2 was found to be 0.0035 kg h^{-1} while the dryer 1 recorded a value of 0.0034 kg h^{-1}. This suggests that the dryer with pebbles performed better than the one without pebbles. Thus, the inclusion of sea pebbles holds promise to enhance heat retention in solar dryers.

4 Conclusion

In conclusion, the results show that the experimental and simulated temperature and relative humidity had a good correlation. Also, the modified designs performed better with a dryer performance coefficient of 1.05 compared to 1.01 of the original design. This occurrence is most likely as a result of the inclusion of the sea pebbles at the collector base and other structural modifications. The modified dryer presents an opportunity for adoption and upscaling to serve as affordable drying facility for farmers and agro-processors in developing countries.

Acknowledgements

Appreciation is extended to the Directorate of Research Innovation and Consultancy, University of Cape Coast in Ghana for providing funds for this work. The authors are also grateful to the original designers of the dryer, Michael Stuart Reid and James Thompson, and the entire Horticulture Innovation Lab team from the University of California, Davis for their support and collaboration.

References

Abano, E. E., H. Ma, and W. Qu. 2011. Influence of air temperature on the drying kinetics and quality of tomato slices. *Journal of Food Processing and Technology*, 2(5): 1-9.

Abano, E. E., and R. S. Amoah. 2015. Microwave and blanch-assisted drying of white yam (*Diascorea rotundata*). *Food Science and Nutrition*, 3(6): 586-596.

Affognon, H., C. Mutungi, P. Sanginga, and C. Borgemeister. 2015. Unpacking postharvest losses in Sub-Sahara Africa: a meta-analysis. *World Development*, 66: 49-68.

Alonge, O. I., and S. O. Obayopo. 2019. Computational Fluid Dynamics and Experimental Analysis of Direct Solar Dryer for Fish. *Agricultural Engineering International: CIGR Journal* 21 (2): 108–17

Bala, B. K., and S. Janjai. 2009 Solar drying of fruits, vegetables, spices, medicinal plants and fish: Developments and Potentials. *International solar food processing conference*, pp. 14-16.

Borah, A., and K. Hazarika. 2017. Simulation and validation of a suitable model of for thin layer drying of ginger rhizomes in an induced draft dryer. *International Journal of Green Energy*, 14(13): 1150-1155.

Deltsidis, A., K. B. Aalia, M. Reid, J. Thompson, E. Mitcham, B. Hansen, M. Bell, B. Dawson, and A. Jarman. 2018. Chimney Solar Dryer Manuel. Available at: hhts://horticulture.ucdavis.edu/information/chimney-solar-dryer-manuel. Accessed 11 02 2020.

Demissie, P., M. Hayelom, A. Kassaye, A. Hailesilassie, M. Gebrehiwot, and M. Vanierschot. 2018. Design, development and CFD modelling of indirect solar food dryer. *Energy Procedia*, 158: 1128-1134.

Deshmukh, A. W., M. N. Varma, C. K. Yoo, and K. L. Wasewar. 2013. Effect of Ethyl oleate pretreatment on drying of ginger: characteristics and mathematical modelling. *Journal of Chemistry*, 2013: 890384.

Engineering ToolBox. 2003. Specific Heat of some common Substances. Available at: https://www.engineeringtoolbox.com/specific-heat-capacityd_391.html. Accessed 3 September 2020.

Goodfellow. 2008. Supplier of materials for research and development. Available at https://www.goodfellow.com/E/Polyethylene-High-density.htm. Accessed 3 September 2020.

Itodo, I. N., J. O. Ijabo, J. A. Charles, N. N. Ezeanaka, and S. O. Akpa. 2019. Performance of deciccent solar crop dryers in Makurdi, Nigeria. *Applied Engineering in Agriculture*, 35(2): 259-270.

Janjai, S., N. Srisittipokakun, and B. Bala. 2008. Experimental and modelling performances of a roof-integrated solar drying system for drying herbs and spices. *Energy*, 33(1): 91-103.

Korsten, L. 2006. Advances in control of postharvest diseases in tropical fresh produce. *International Journal of Postharvest Technology and Innovation*, 1(1): 48-61.

Kumar, D. K., H. Basavaraja, and S. B. Mahajanshetti. 2006. An economic analysis of post-harvest losses in vegetables in Karnataka. *Indian Journal of Agricultural Economics*, 61(1):134-146

Kumi, F., J. Ampah, R. S. Amoah, A. H. Andoh-Odoom, and M. Kodua. 2020. Performance Evaluation of chimney solar dryer for habanero pepper (*Capsicum chinense Jacq*). *African Journal of Food, Agriculture, Nutrition and Development*, 20(4): 16029-16045.

Odinaka, N. B., and G. U. Akubue. 2018. Computational fluid dynamic performance analysis of mixed mode solar dryer. *International Journal of Scientific & Engineering Research* 9 (6): 133–44.

Poonia, S., A. K. Singh, P. Santra, and D. Jain. 2019. Economic analysis of inclined solar dryer for drying of fruit and vegetables. *International Journal of Agriculture Science*, 11(20): 9154-9159.

Sanghi, A., R. P. K. Ambrose, and D. Maier. 2018. CFD

Simulation of corn drying in a natural convection solar dryer. *Drying Technology*, 36(7): 859-870.

Sheahan, M., and C. B. Barret. 2017. Review: Food loss and waste in Sub-Saharan Africa. *Food Policy*, 70: 1-12.1

Shitanda, D., and N. V. Wanjala. 2006. Effect of different drying methods on the quality of jute (*Corchorus ohtorius* L.). *Drying Technology*, 24(1): 95-95.

Turhan, M., K. N. Turhan, and F. Sahbaz. 1997. Drying kinetics of red pepper. *Journal of Food Processing and Preservation*, 21(3): 209-223.